Repetitive amiodarone administration causes liver damage via adipose tissue ER stress-dependent lipolysis, leading to hepatotoxic free fatty acid accumulation

Hubel, Einav

2021-09

Hubel , E , Fishman , S , Holopainen , M , Käkelä , R , Shaffer , O , Houri , I , Zvibel , I & Shibolet , O 2021 , ' Repetitive amiodarone administration causes liver damage via adipose tissue ER stress-dependent lipolysis, leading to hepatotoxic free fatty acid accumulation ' , American Journal of Physiology: Gastrointestinal and Liver Physiology , vol. 321 , pp. G298-G307 . https://doi.org/10.1152/ajpgi.00458.2020

http://hdl.handle.net/10138/346177
https://doi.org/10.1152/ajpgi.00458.2020

unspecified
acceptedVersion

Repetitive amiodarone administration causes liver damage via adipose tissue ER-stress dependent lipolysis, leading to hepatotoxic free fatty acid accumulation

Running title: Amiodarone induces hepatic free fatty acid accumulation

Einav Hubel[1], Sigal Fishman[1,2], Minna Holopainen[3,4], Reijo Käkelä[3,4], Ortal Shaffer[5], Inbal Houri[1,2], Isabel Zvibel[1] #, Oren Shibolet[1,2] #.

1. The Research Center for Digestive Tract and Liver Diseases, Tel-Aviv Sourasky Medical Center and the Sackler Faculty of Medicine, Tel-Aviv University, Tel-Aviv, Israel.

2. Department of Gastroenterology and Hepatology, Tel-Aviv Sourasky Medical Center, Tel-Aviv, Israel.

3. Helsinki University Lipidomics Unit (HiLIPID), Helsinki Institute for Life Science (HiLIFE) and Biocenter Finland, Helsinki, Finland

4. Molecular and Integrative Biosciences Research Programme, Faculty of Biological and Environmental Sciences, University of Helsinki, Helsinki, Finland

5. Surgery department, Tel-Aviv Sourasky Medical Center, Tel-Aviv, Israel.

Equal senior authors.

Corresponding author: Oren Shibolet MD, Liver Unit, Department of Gastroenterology, Tel-Aviv Medical Center and Tel-Aviv University, Tel-Aviv, Israel; Tel: 972-3-6973984; Fax: 972-3-6966286. Email: orensh@tlvmc.gov.il

Figures: 6

Supplementary material: 1 Table

Acknowledgements: This work was supported by the German Israeli Fund grant # I-1188-74.9/2012 to O.S and H.B and the Israel Science Foundation grant # 970/12 to O.S. The authors thank Sanna P. Sihvo (HiLIPID) for excellent technical assistance.

Authors contributions: EH, OS, IH and RA performed the experiments, MH performed the fatty acid analysis, EH, MH, RK and IZ analyzed the data, SF, IZ and OS wrote the paper, which was edited and approved by all authors.

Conflict of interest: The authors declare no conflict of interest.

Data availability statement: The data that support the findings of this study are available from the corresponding author upon reasonable request. Some data may not be made available because of privacy or ethical restrictions.

Abstract

Drug-induced liver injury is an emerging form of acute and chronic liver disease that may manifest as fatty liver. Amiodarone (AMD), a widely used anti-arrhythmic drug, can cause hepatic injury and steatosis by a variety of mechanisms, not all completely understood. We hypothesized that repetitive AMD administration may induce hepatic lipotoxicity not only via effects on the liver, but also via effects on adipose tissue. Indeed, repetitive AMD administration induced endoplasmic reticulum (ER) stress in both liver and adipose tissue. In adipose tissue, AMD reduced lipogenesis and increased lipolysis. Moreover, AMD treatment induced ER stress and ER stress-dependent lipolysis in 3T3L1 adipocytes *in vitro*. In the liver, AMD caused increased expression of genes encoding proteins involved in fatty acid (FA) uptake and transfer (*Cd36*, *Fabp1* and *Fabp4*) and resulted in increased hepatic accumulation of free FAs, but not of triacylglycerols. In line with this, there was increased expression of hepatic *de novo* FA synthesis genes. However, AMD significantly reduced the expression of the desaturase *Scd1* and elongase *Elovl6*, detected at mRNA and protein levels. Accordingly, the FA profile of hepatic total lipids revealed increased accumulation of palmitate, a SCD1 and ELOVL6 substrate, and reduced levels of palmitoleate and *cis*-vaccenate, products of the enzymes. In addition, AMD-treated mice displayed increased hepatic apoptosis.

The studies show that repetitive AMD induces ER stress and aggravates lipolysis in adipose tissue, while inducing a lipotoxic hepatic lipid environment, suggesting that AMD-induced liver damage is due to compound insult to liver and adipose tissue.

Key words: drug-induced liver injury, amiodarone, lipogenesis, ER stress, lipolysis.

New & Noteworthy

AMD chronic administration induces hepatic lipid accumulation by several mechanisms, including induction of hepatic ER stress, impairment of B-oxidation and inhibition of triacylglycerol secretion.

Our study shows that repetitive AMD treatment induces not only hepatic ER stress, but also adipose tissue ER stress and lipolysis and hepatic accumulation of free fatty acids and enrichment of palmitate in the total lipids.

Understanding the toxicity mechanisms of AMD would help devise ways to limit liver damage.

Introduction

Amiodarone (AMD) is a class III anti-arrhythmic drug, used for the treatment and prevention of both ventricular and atrial arrhythmias. Its primary mechanism of action in the heart is the blocking of potassium channels, but it can also block sodium and calcium channels and the beta and alpha-adrenergic receptors. AMD use is associated with various adverse effects, among them hepatotoxicity (1). Approximately 25% of patients treated with the drug have elevated liver enzymes, and 3% develop “symptomatic” hepatitis (2,3). There are two clinical forms of AMD hepatotoxicity. Severe acute hepatitis develops within 24 hours after intravenous (IV) infusion (4). Chronic toxicity, following long-term oral therapy, usually involves mild asymptomatic elevation of aminotransferases (5). The pathogenesis of long-term AMD-induced steatosis and liver injury remains unclear. One suggested mechanism is the accumulation of triacylglycerols (TAGs) via inhibition of mitochondrial β-oxidation of fatty acids (FAs) (6). There is evidence that AMD disrupts hepatic lipoprotein secretion via inhibition of microsomal TAG transfer protein (MTP) activity, thus decreasing ApoB-dependent VLDL secretion (7). Another suggested mechanism of AMD-induced steatohepatitis is via induction of endoplasmic reticulum (ER) stress. The ER is the cellular site for protein folding and lipid transport. ER stress occurs when the load of unfolded proteins exceeds the ER folding capacity, and induces a reaction to re-establish the homeostasis (8). This reaction is termed the unfolded protein response (UPR) and involves activation of several pathways including aberrations of lipid metabolism and trafficking by the ER (9). ER stress signaling is regulated by the key molecular chaperone Grp 78 (glucose-regulated protein 78kDa, also known as Bip). When misfolded proteins accumulate in the ER, Grp78 is sequestered, initiating the UPR. Three major ER stress sensors, IRE1, PERK and ATF6, transduce the mammalian UPR. IRE1 and PERK are activated by autophosphorylation, while ATF6 is activated by intra-

membrane cleavage. Activated IRE1 splices the mRNA of XBP1 yielding the potent transcription factor XBP1s, inducing cellular stress responses and activating the immune system. Activated PERK phosphorylates eIF2α, inducing selective transcription of *Atf4*, *Atf3* and *Ddit3* in a sequential manner. Activation of the UPR leads initially to attenuation of protein synthesis and protein translocation into the ER, preventing further misfolding, followed by an increase in ER folding capacity. If the stress is not relieved, cell death is triggered, mediated to prevent the damaging effect of misfolded proteins (10). While acute ER stress leads to apoptosis, chronic sub-lethal ER stress causes cellular adaptation and resistance to apoptosis (11). ER stress/UPR activation has been reported in most models of hepatic steatosis and contributes to lipid accumulation and lipotoxicity (12). Using a mouse model of acute AMD treatment, we detected liver damage and lipid accumulation, accompanied by activation of ER stress/UPR (13). Importantly, AMD-induced lipid accumulation was not mediated by *de novo* hepatic lipogenesis, increased adipose tissue lipolysis or increased hepatic uptake of TAG or free FA (FFA). Rather, AMD strongly increased hepatic mRNA expression of lipid droplet proteins, particularly Cidea and Cidec, suggesting a possible link between ER stress and increased TAG storage.

In the present study, we investigated the mechanism of repetitive AMD-induced liver injury, which may have a different mechanism from the acute injury. Induction of ER stress in adipose tissue has been documented to induce lipolysis and increase levels of circulating FFAs (14,15). Several studies have demonstrated that pharmacological inhibition of adipose tissue lipolysis with synthetic long chain FAs or deletion of adipose tissue lipase (ATGL) in mice protects from development of hepatic ER stress (16, 17). This suggests that drug-induced ER stress in the adipose tissue could affect hepatic ER stress

and lipotoxicity. However, this avenue of research has not yet been explored in a drug-induced liver injury (DILI) model.

Based on the hypothesis that AMD induces ER stress not only in the liver, but also in adipose tissue, we have found a novel pathway of AMD-induced liver lipotoxicity. In this pathway, increased lipolysis in adipose tissue results in enhanced circulating FFAs, which are then taken up by the liver and together with increased *de novo* lipogenesis lead to hepatotoxicity, liver injury and inflammation.

Methods

Cell culture

The 3T3L1 cell line was obtained from the American Type Culture Collection (ATCC, CL -173) and cultured in DMEM (high glucose) supplemented with 10% Bovine Calf Serum (BCS) (Biological Industries), 100 U/ml penicillin, 100 mg/ml streptomycin in a 5% CO_2 humidified atmosphere and allowed to reach 70% confluence. Cells were then seeded at a density of $3x10^3$ cells/cm^2 in DMEM + 10%BCS and allowed to reach 70% confluency. To initiate differentiation, cells were cultured in DMEM with 10% BCS, IBMX (0.5 mM), dexamethasone (1 µM) and insulin (10µg/ml) for 3days. The medium was changed to DMEM with 10% FCS and insulin (10µg/ml). Medium was changed every 3 days. By day 10, fully differentiated adipocytes were obtained. Adipocytes were treated with 100µM AMD with or without 50µM of an ER stress inhibitor (BIX)(Sigma) for 8h. Medium was collected for testing lipolysis and cells were harvested for RNA extraction. Experiments were repeated three times.

Animals and experimental protocol

All animal care and experimental protocols use of animals was approved by the TASMC Animal Use and Care Committee (Ethical Approval Numbers 8-1-16, 12-6-17). Wild type (WT) C57BL/6JOlaHsd mice (Envigo) were maintained in the animal facility of the Tel Aviv Sourasky Medical Center on a standard rodent chow diet fed ad libitum, kept under controlled temperature of 22‑24°C and 12h light-dark cycles. We used 10 weeks old male mice weighting 24–26g. Mice were randomly divided into three groups, mice receiving saline by gavage for 4 days, mice receiving acute AMD treatment and mice receiving repetitive AMD treatment. For the acute model of AMD injury, mice were injected

intraperitoneally (i.p.) with 250mg.kg^{-1} body weight AMD-HCl (AMD) (Sanofi Winthrop Industrie, France) (13). For the repetitive model of AMD injury, mice received daily gavage with vehicle (saline) or 180mg.kg^{-1} body weight of AMD for four consecutive days. The sample size in each group was determined based on our previous studies with similar experimental protocols. The number of animals for each analysis is described in the figure legends. In vivo experiments were repeated four times.

Analysis of serum and liver metabolic markers

Mouse serum was collected and kept in -80°C until assessed. Serum and liver triglycerides (TG), liver enzymes ALT and AST were measured using the Advia 2000 Automatic Analyzer. Total free fatty acids (FFA) concentrations in serum and liver were measured by ELISA (Abcam, ab65341).

Oil Red O staining

Oil Red O (ORO) (Sigma Aldrich USA #O1391) was issolved in propylene glycol (1% weight/volume). Frozen sections were fixed in 4% formaldehyde for 10 min, followed by three washes for 30 sec in double distilled water (DDW). Slides were subjected to 100% polyethylene glycol (PEG) for 2 min followed by 15 min incubation with ORO. Then, slides were subjected to 60% PEG for 1 min, followed by three washes in tap water. Slides were stained with Gill III Hematoxylin for 1 min and washed three times with DDW. Cover slips were mounted with glycerol.

TUNEL assay

Livers of control and AMD- treated mice were fixed in formalin and embedded in paraffin. Liver sections of 5μm were used to assess apoptosis with Dead End fluorimetric TUNEL system (Promega), as previously described (18).

Lipolysis assay

Differentiated 3T3-L1 adipocytes were treated with 100μM AMD with or without 50μM Bix and with 10μM isoproterenol as positive control for 8h in medium with no phenol. Media were collected and tested for free glycerol using an ELISA kit for glycerol (Abcam, ab65337).

Western blot analysis

Western blot analysis was performed as previously described (Uzi et al, 2013). Total protein from liver was extracted by homogenization in ice-cold RIPA buffer (PBS, 1% Igepal, 0.5% sodium deoxycholate, 0.1% sodium dodecyl sulfate, protease and phosphatase inhibitors cocktails 1:100). After centrifuging at 12,000 *g* for 15 min at 4°C, the protein concentration was determined using a Protein Assay Dye Reagent concentrate (Bio-Rad Laboratories, USA). Proteins were separated by SDS-PAGE, blotted onto cellulose nitrate membranes (Whatman, Protran BA-83) and blots were blocked for 1 h in Tris-Tween buffered saline (TTBS) with 5% milk. Blots were incubated overnight at 4°C with primary antibodies and then incubated with horseradish peroxidase-conjugated secondary antibodies and subjected to chemi-luminescent detection using the Micro Chemiluminescent imaging system (DNR Bio Imaging Systems). Densitometry was performed using the Image J software and expression of proteins normalized to expression of housekeeping gene p97.

Quantitative RT-PCR

Total RNA was extracted from isolated livers using TriReagent (Sigma) and from epididymal adipose tissue using Qiazol and Lipid RNA extraction kit (Qiagen). Total RNA was reverse-transcribed using the High capacity cDNA RT kit (Applied Biosystems). Real time qRT-PCR was performed with the Fast SYBR Green Master

Mix (Applied Biosystems) using the Corbett rotor light cycler. Quantification of the PCR signals of each sample was performed by the ΔCt method normalized to *Rplp0* housekeeping genes. The primer sequences are shown in **Supplementary Table S1 (**DOI 10.6084/m9.figshare.14837640).

Hepatic and serum fatty acid profile analysis

The FA composition of liver and serum samples was determined with gas chromatography (GC). The liver samples were homogenized and serum samples evaporated near to dryness before the transmethylation according to the recommendations of Christie (19) and as described previously (20). In brief, samples were heated with 1% H_2SO_4 in methanol under nitrogen, and the formed FA methyl esters were extracted in two steps with hexane. The samples were dried overnight in anhydrous Na_2SO_4 and concentrated. The FA methyl esters were identified with GCMS-QP2010 Ultra (Shimadzu Scientific Instruments, Kyoto, Japan) with mass selective detector (MSD) and quantified using Shimadzu GC-2010 Plus with flame-ionization detector (FID), both equipped with a Zebron ZB-wax capillary column (30 m, 0.25 mm ID and film thickness 0.25 μm; Phenomenex, Torrence CA, USA). The FA proportions were expressed as mol%, and the FAs were marked using the following abbreviations: [carbon number]: [number of double bonds] n-[position of the first double bond calculated from the methyl end] (e.g., 16:1n-7 for palmitoleate).

Data and Statistical analysis

Randomization was used to assign mice to the experimental groups and treatment conditions for the *in vivo* studies. Data are expressed as the mean ± SEM. Statistical significance among groups was assessed by ANOVA, followed by a Bonferroni post hoc analysis using GraphPad Prism v5 for Windows (San Diego, CA; RRID:SCR_002798). Post hoc tests were conducted only if F was significant, and there was no variance

inhomogeneity. For analysis of statistical significance between two groups we used a two-tailed student t-test. Significance was set at $p < .05$.

Materials

Amiodarone AMD-HCl (AMD) was purchased from Sanofi Winthrop Industrie, France. BIX was from Sigma. The primary antibodies used were: SCD1 (Abcam, ab39969), ELOVL6 (Abcam, ab69857), FAS (Santa Cruz Biotechnology, sc-20140), pEIF2 (Cell Signaling #119A11), pIRE1α (Abcam USA, ab48187), Bip (Abcam, ab21685), C/EBP homologous protein (CHOP) (Cell Signaling, #2895), pJNK (Cell Signaling, #9251), pHSL (Cell Signaling, S660), CD36 (Abcam, ab133625), housekeeping P97 (rabbit polyclonal prepared in the lab of prof. Boaz Tirosh, Hebrew University, Jerusalem).

Results

We have previously shown that acute AMD administration induces hepatic ER stress and hepatic steatosis (13). We now established a model of liver damage induced by repetitive AMD administration, which would be more similar to human liver damage, which is caused by long term-treatment with AMD. Based on previous publications, AMD administration by gavage for 4 days had the same effect on liver damage as a more prolonged administration for 11 days (21). In the present study, the 4–day regimen of AMD administration by gavage led to significantly increased levels of liver enzymes alanine aminotransferase (ALT) and aspartate aminotransferase (AST), and also caused hepatic lipid accumulation (Figure 1a and 1b). Hence, the model of 4–day administration enables us to study a more chronic form of liver injury. We next determined the expression of ER stress markers induced by repetitive administration of AMD. As in mice with acute treatment with AMD (13), repetitive AMD administration strongly induced *Atf3*, *Atf4*, *Bip*, *Erdj4* and *Dnajc3*, but not *Ddit3* (Figure 1c). Analysis of ER stress sensors revealed increased phosphorylation of EIF2α and IRE1 after repetitive AMD treatment (Figure 1d). These data show that repetitive AMD induces strong hepatic ER stress and damage.

Repetitive AMD induces adipose tissue ER stress and lipolysis, but inhibits lipogenesis

Long-term treatment with AMD leads to its accumulation in adipose tissue (22-24). We therefore assessed whether AMD induces ER stress simultaneously in liver and epididymal adipose tissue (epiWAT), a part of the whole visceral fat. We first evaluated the effect of acute versus repetitive AMD administration on expression of ER stress markers in adipose tissue. Acute AMD slightly increased expression of *Atf3* and *Atf4*, whereas repetitive AMD strongly enhanced the expression of these transcription factors, in addition to increasing

expression of *Bip*, *Ddit3* and *Erdj4* (Figure 2a). We further assessed markers of ER stress and UPR in adipose tissue following repetitive AMD treatment. Western blot analysis revealed increased levels of ER sensors, phosphorylated pIRE1α, and phosphorylated EIF2α in adipose tissue of AMD treated mice (Figure 2b). Protein levels of Bip and CHOP (encoded by *Ddit3* gene) were also induced following AMD treatment (Figure 2b). Adipose tissue also displayed increased phosphorylation of JNK (Figure 2b), as well as strongly increased expression of its downstream target *Tnfa* (Figure 2c).

Previous studies have documented that ER stress in adipocytes *in vitro* or in adipose tissue *in vivo* induces lipolysis (14, 15, 25). Accordingly, following AMD administration we observed increased levels of phosphorylated hormone sensitive lipase (pHSL), the rate-limiting enzyme regulating lipolysis (Figure 3a). In line, serum levels of FFAs were increased in the AMD-treated mice (Figure 3b). When addressing the saturated fatty acids (SFAs) and monounsatured fatty acids (MUFAs) in gas chromatographic FA profiles of serum, we found that the relative concentrations of oleate (18:1n-9) and *cis*-vaccenate (18:1n-7) were lower in the AMD group than in the controls (Figure 3c). This observation can be explained by reduced expression of the desaturase *Scd1*, which converts stearate (18:0) to 18:1n-9 and palmitate (16:0) to palmitoleate (16:1n-7), further elongated to 18:1n-7 (Figure 3d). We further examined levels of lipogenesis enzymes FAS, ELOVL6 and SCD1, and observed significantly reduced FAS and ELOVL6 in the adipose tissue of AMD-treated mice, but similar levels of SCD1 (Figure 3e). Collectively, these results show that repetitive AMD induces ER stress and lipolysis in adipose tissue and inhibits lipogenesis.

AMD treatment induces ER stress and lipolysis in 3T3L1 differentiated adipocytes *in vitro*

We wanted to validate that AMD induces ER-stress dependent lipolysis in adipocytes. For this purpose, we differentiated 3T3L1 cells into adipocytes and treated them with different concentrations of AMD for 8 h, in order to determine the best concentration for induction of ER stress (Figure 4a). We found that 100 μM AMD was the lowest concentration to produce increased expression of all ER stress markers (Figure 4a). Therefore, we next investigated the effect of concentration on ER stress in adipocytes after 8, 24 and 48 h. We found that optimal ER stress was induced after 8 h of treatment (Figure 4b). In order to determine whether BIX, an ER stress inhibitor, reduced AMD-induced ER stress in 3T3L1 adipocytes, we treated the cells for 8 h with 100 μM AMD, with or without 50 μM BIX, and found that the AMD-induced expression of *Atf4*, *Bip*, *Erdj4* and *Dnajc3*, but not *Atf3*, was abolished in the presence of BIX (Figure 4c). ATF3 is a factor induced by several types of stress, including ER stress (*Hai et al*, 2010). Since inhibition of ER stress with Bix does not alleviated Atf3 expression, it indicates that AMD induces this transcription factor via a different mechanism.

Finally, we assessed whether AMD-induced ER stress-dependent lipolysis in 3T3L1 differentiated adipocytes. AMD induced modest, albeit statistically significant, lipolysis, which was abolished in the presence of ER stress inhibitor BIX (Figure 4d).

Repetitive AMD induces hepatic FFA, but not TAG, accumulation.

In our repetitive AMD mouse model, serum TAG level was significantly reduced, as expected, since AMD prevents TAG secretion by inhibiting the microsomal transfer protein that induces lipidation of ApoB and VLDL secretion (7) (Figure 5a). Surprisingly, the hepatic TAG level was similar in the AMD and control groups. In contrast, significant accumulation of FFA was found in the AMD group (Figure 5b-c). The liver can internalize and traffic serum FFAs via several cell surface molecules, such as CD36 and FA binding

protein 4 (FABP4) (26). RT-PCR analysis showed significantly increased expression of both *Cd36* and *Fabp4* following repetitive AMD treatment (Figure 5d). In addition, protein levels of CD36 were also increased in the livers of AMD-treated mice (Figure 5e). Altogether, the results suggest increased uptake and accumulation of FFA in the liver.

AMD induces genes involved in hepatic FFA synthesis, but inhibits expression of elongation and desaturation genes leading to hepatic palmitate accumulation and apoptosis

Liver FFAs (like the FAs subsequently incorporated into hepatic lipids) may originate not only from circulating lipoproteins or adipose tissue but also from hepatic *de novo* lipogenesis. Therefore, we next examined hepatic expression of lipogenesis-related genes. This analysis revealed that AMD significantly induced the expression of master lipogenesis transcription factor *Srebp1* and its downstream target *Fasn* (Figure 6a). However, hepatic expression of the elongation and desaturation genes *Elovl6* and *Scd1* was significantly inhibited by AMD treatment (Figure 6a). Western blot analysis of FAS, SCD1 and ELOVL6 further demonstrated upregulation of FAS and downregulation of SCD1 and ELOVL6 in the livers of the AMD-treated group (Figure 6b).

We assessed hepatic lipid profile, using 16:0 as the substrate, the product of ELOVL6 is 18:0 and that of SCD1 is 16:1n-7. The 18:1n-9 is produced from 16:0 by ELOVL6 and SCD1, whereas the 18:1n-7 is produced when these enzymes act in reverse order. Inhibition of these enzymes would lead to hepatic accumulation of the ELOVL6 substrate 16:0. Indeed, the hepatic FA profile showed relative increase of the FAS product 16:0 and reduced relative concentrations of the SCD1 product 16:1n-7 and the ELOVL6 and SCD1 product 18:1n-7 (Figure 6c). Moreover, livers of AMD-treated mice displayed increased apoptosis (Figure 6d).

Discussion

AMD is a commonly used anti-arrhythmic drug known to induce both acute and chronic liver damage hallmarked by steatosis. The present study shows that while acute AMD treatment induces ER stress in the liver, repetitive AMD administration induces even stronger ER stress in both liver and adipose tissue. Moreover, repetitive AMD administration increases adipose tissue lipolysis. We found that in the model of repetitive administration of AMD, there is increased hepatic accumulation of FFAs, but not of TAGs. This increase in FFAs may be due both to uptake of serum FFAs and to the increased FA synthesis observed in the liver. Interestingly, AMD treatment resulted in dramatically reduced expression of SCD1 in adipose tissue and liver, and ELOVL6 in liver, leading to increased relative concentrations of hepatic 16:0, the substrate for SCD1 and ELOVL6. With respect to the *in vivo* induction of ER stress by AMD in liver and adipose tissue, we cannot discount the possibility of indirect effects causing ER stress in these tissues.

The phenomenon of ER stress-induced lipolysis in adipose tissue or adipocytes has been described by several groups (14, 15, 25). In the present work, we show that repetitive AMD treatment induces adipose tissue ER stress and ER stress-dependent lipolysis. We show that AMD induces lipolysis in 3T3L1 adipocytes, and this effect is abolished in the presence of the ER stress inhibitor BIX.

Our previous study showed that acute AMD treatment stimulated hepatic lipid accumulation, despite strongly attenuated *de novo* lipogenesis (13). In the present study, a four day treatment with AMD stimulated hepatic expression of lipid uptake and transport proteins CD36 and FABP4. Interestingly, while the hepatic expressions of lipogenesis master transcription factor SREBP1c and its downstream target FASN are increased in AMD-treated mice, the expression of genes encoding elongation and desaturation enzymes

ELOVL6 and SCD1 is strongly attenuated. In line with these changes of enzyme expression, the hepatic FA profiles revealed that AMD-treated mice had more of the hepatotoxic ELOVL6 and SCD1 substrate 16:0 and less of their products 16:1n-7 and 18:1n-7. Of note, *Scd1* expression was also strongly attenuated in adipose tissue of AMD-treated mice, but there were similar levels of SCD1 protein in control and AMD-treated groups.

The liver protects itself from lipotoxicity by directing incoming FFA from the serum and from *de novo* lipogenesis to synthesis of TAG, which is then stored in lipid droplets (26). The hallmark of the steatotic liver is accumulation of TAG. However, during the development of further liver injury and inflammation and progress to steatohepatitis, FFA, ceramides and free cholesterol also accumulate (27). The elongation and desaturation of FAs, taken up from serum or *de novo* synthesized by liver, are essential for the generation of TAG (28, 29). The ELOVL6 elongates 16:0 to 18:0, and SCD1 catalyzes desaturation of these SFAs to the respective MUFAs 16:1n-7 and 18:1n-9. These MUFAs are the preferential substrates for TAG synthesis. Genetic or pharmacological inhibition of SCD1 sensitizes cells to SFA-induced apoptosis (30). Furthermore, mice with liver-specific SCD1 deficiency have been reported to be protected from high carbohydrate diet-induced obesity and insulin resistance (31). The 16:0 is a known inducer of both ER stress, mitochondrial damage and hepatic apoptosis (32,33). We did not determine mitochondrial damage in our study, however, the enrichment of 16:0 observed in the AMD-treated mice was accompanied by hepatic ER stress and apoptosis in these mice and could cause these effects.

Several signals have been shown to down-regulate transcription of SCD1. First, activation of TLR-TRIF-IRF3 pathway inhibits SCD1 expression (34). Second, overexpression of

transcription cofactor BTG1 (B cell translocation gene 1) suppresses activity of transcription factor ATF4, which leads to reduced SCD1 transcription (35). Third, hepatic leptin signaling via Erk1/2 attenuates SCD1 mRNA (36). Interestingly, it appears that SCD1 deficiency induces ER stress/UPR via upregulation of PGC1α and activation of mTORC1 (37). In contrast with increased hepatic FA synthesis, AMD-treated mice displayed reduced expression of *de novo* lipogenesis enzymes (FASN and SCD1) and their serum FA profiles with reduced 18:1n-9 and 18:1n-7 reflected the reduced expression of SCD1.

In conclusion, we show that repetitive AMD administration causes unique metabolic aberrations in liver and adipose tissue. Both contribute to hepatic lipotoxicity through accumulation of FFA and reduced FA desaturation.

References

1. Greene HL, Graham EL, Werner JA, Sears GK, Gross BW, Gorham JP, Kudenchuk PJ, Trobaugh GB. Toxic and therapeutic effects of amiodarone in the treatment of cardiac arrhythmias. *J Am Coll Cardiol*. 2(6):1114-28.2, 1983.

2. **Lewis JH, Ranard RC, Caruso A, Jackson LK, Mullick F, Ishak KG, Seeff LB, Zimmerman HJ**. Amiodarone hepatotoxicity: prevalence and clinicopathologic correlations among 104 patients. *Hepatology*. 9(5):679-85, 1989.

3. **Vassallo P, Trohman RG.** Prescribing AMD: an evidence-based review of clinical indications. *J Am Med Assoc* 298:1312-22, 2007.

4. **Nasser M, Larsen TR, Waanbah B, Sidiqi I, McCullough PA**. Hyperacute drug-induced hepatitis with intravenous AMD: case report and review of the literature. *Drug Healthc Patient Saf.* 5:191-8, 2013.

5. **Adams PC, Holt DW, Storey GC, Morley AR, Callaghan J, Campbell RW** . AMD and its desethyl metabolite: tissue distribution and morphologic changes during long-term therapy. *Circulation*. 72:1064-75, 1985.

6. **Begriche K, Massart J, Robin MA, Borgne-Sanchez A, Fromenty B**. Drug induced toxicity on mitochondria and lipid metabolism: mechanistic diversity and deleterious consequences for the liver. *J Hepatol*. 54:773-94, 2011.

7. **Letteron P, Sutton A, Mansouri A, Fromenty B, Pessayre D.** Inhibition of microsomal triglyceride transfer protein: another mechanism for drug-induced steatosis in mice. *Hepatology* 38:133-40, 2003.

8. **Ron D, Walter P**. Signal integration in the endoplasmic reticulum unfolded protein response. *Nat Rev Mol Cell Biol* 8:519-29. 2007.

9. **Almanza A, Carlesso A, Chintha C, Creedican S, Doultsinos D, Leuzzi B, Luís A, McCarthy N, Montibeller L, More S, Papaioannou A, Püschel F, Sassano ML, Skoko J, Agostinis P, de Belleroche J, Eriksson LA, Fulda S, Gorman AM, Healy S, Kozlov A, Muñoz-Pinedo C, Rehm M, Chevet E, Samali A.** Endoplasmic reticulum stress signalling - from basic mechanisms to clinical applications. *FEBS J*. 286(2):241-278, 2019.

10. **Szegezdi E, Logue SE, Gorman AM, Samali A.** Mediators of endoplasmic reticulum stress-induced apoptosis. *EMBO Rep* 7:880-5, 2006.

11. **Rutkowski DT, Arnold SM, Miller CN, Wu J, Li J, Gunnison KM, Mori K, Sadighi Akha AA, Raden D, Kaufman RJ.** Adaptation to ER stress is mediated by differential stabilities of pro-survival and pro-apoptotic mRNAs and proteins. *PLoS Biology* 4:e374, 2006.

12. **Puri P, Mirshahi F, Cheung O, Natarajan R, Maher JW, Kellum JM, Sanyal AJ.** Activation and dysregulation of the unfolded protein response in nonalcoholic fatty liver disease. *Gastroenterology* 134:568-76, 2008.

13. **Erez N, Hubel E, Avraham R, Cohen R, Fishman S, Bantel H, Manns M, Tirosh B, Zvibel I, Shibolet O.** Hepatic AMD Lipotoxicity Is Ameliorated by Genetic and Pharmacological Inhibition of Endoplasmatic Reticulum Stress. *Tox Sci*. 159: 402-412, 2017.

14. **Deng J, Liu S, Zou L, Xu C, Geng B, Xu G**. Lipolysis response to endoplasmic reticulum stress in adipose cells. *J Biol Chem*. 287:6240-9, 2012.

15. **Bogdanovic E, Kraus N, Patsouris D, Diao L, Wang V, Abdullahi A, Jeschke MG**. Endoplasmic reticulum stress in adipose tissue augments lipolysis. *J Cell Mol Med*. 19(1):82-91, 2015.

16. Fuchs CD, Claudel T, Kumari P, Haemmerle G, Pollheimer MJ, Stojakovic T, Scharnagl H, Halilbasic E, Gumhold J, Silbert D, Koefeler H, Trauner M. Absence of adipose triglyceride lipase protects from hepatic endoplasmic reticulum stress in mice. *Hepatology*. 56(1):270-80.28, 2012.

17. **Kalderon B, Azazmeh N, Azulay N, Vissler N, Valitsky M, Bar-Tana J**. Suppression of adipose lipolysis by long-chain fatty acid analogs. *J Lipid Res*. 53:868-78, 2012.

18. **Hubel E, Saroha A, Park WJ, Pewzner-Jung Y, Lavoie EG, Futerman AH, Bruck R, Fishman S, Dranoff JA, Shibolet O, Zvibel I.** Sortilin Deficiency Reduces Ductular Reaction, Hepatocyte Apoptosis, and Liver Fibrosis in Cholestatic-Induced Liver Injury. *Am J Pathol*.187:122-133, 2017.

19. **Christie WW**. Preparation of ester derivatives of fatty acids for chromatographic analysis. In: *Advances in Lipid Methodology*. Editor WW Christie - Two, Oily Press, Dundee, Scotland, 1993, p. 69–111.

20. **Käkelä R, Käkelä A, Kahle S, Becker BH, Kelly A, Furness RW**. Fatty acid signatures in plasma of captive herring gulls as indicators of demersal or pelagic fish diet, *Mar. Ecol. Prog. Ser.* 293: 191-200, 2005.

21. **Vitins AP, Kienhuis AS, Speksnijder EN, Roodbergen M, Luijten M, van der Ven LT**. Mechanisms of AMD and valproic acid induced liver steatosis in mouse in vivo act as a template for other hepatotoxicity models. *Arch Toxicol*. 88:1573-88, 2014.

22. **Brien JF, Jimmo S, Brennan FJ, Ford SE, Armstrong PW.** Distribution of AMD and its metabolite, desethylAMD, in human tissues. *Canadian Journal of Physiology and Pharmacology* 65:360-4, 1987.

23. **Plomp TA, Hauer RN, Robles de Medina EO**. AMD and desethylAMD concentrations in plasma and tissues of surgically treated patients on long-term oral AMD treatment. *In Vivo.* 4:97-100, 1990.

24. **Wyss PA, Moor MJ, Bickel MH**. Single-dose kinetics of tissue distribution, excretion and metabolism of AMD in rats. *J Pharmacol Exp Therapeutics*. 254:502-7, 1990.

25. **Wang L, Zhang B, Huang F, Liu B, Xie Y**. Curcumin inhibits lipolysis via suppression of ER stress in adipose tissue and prevents hepatic insulin resistance. *J Lipid Res*. **57**:1243-55, 2016.

26. **Canbay A, Bechmann L, Gerken G**. Lipid metabolism in the liver. *Z Gastroenterologie* 45:35-41, 2007.

27. **Svegliati-Baroni G, Pierantonelli I, Torquato P, Marinelli R, Ferreri C, Chatgilialoglu C, Bartolini D, Galli F.** Lipidomic biomarkers and mechanisms of lipotoxicity in non-alcoholic fatty liver disease. *Free Rad Biol Med*. **144**:293-309, 2019.

28. **AlJohani AM, Syed DN, Ntambi JM**. Insights into Stearoyl-CoA Desaturase-1 Regulation of Systemic Metabolism. *Trends Endocrinol Metab*. 28(12):831-842, 2017.

29. **Guillou H, Zadravec D, Martin PG, Jacobsson A**. The key roles of elongases and desaturases in mammalian fatty acid metabolism: Insights from transgenic mice. *Prog Lipid Res*. 49:186–199, 2010.

30. **Li ZZ, Berk M, McIntyre TM, Feldstein AE.** Hepatic lipid partitioning and liver damage in nonalcoholic fatty liver disease: role of stearoyl-CoA desaturase. *J Biol Chem*. 284:5637–5644, 2009.

31. **Miyazaki M, Flowers MT, Sampath H, Chu K., Otzelberger C, Xueqing Liu X, Ntambi JM**. Hepatic stearoyl-CoA desaturase-1 deficiency protects mice from carbohydrate-induced adiposity and hepatic steatosis. *Cell Metab* 6, 484–496, 2007.

32. **Chen X, Li L, Liu X, Luo R, Liao G, Li L, Liu J, Cheng J, Lu Y, Chen Y** .Oleic acid protects saturated fatty acid mediated lipotoxicity in hepatocytes and rat of non-alcoholic steatohepatitis. *Life Sci*. 203:291-304, 2018.

33. **Pfaffenbach KT, Gentile CL, Nivala AM, Wang D, Wei Y, Pagliassotti MJ**. Linking endoplasmic reticulum stress to cell death in hepatocytes: roles of C/EBP homologous protein and chemical chaperones in palmitate-mediated cell death. *Am J Physiol Endocrinol Metab*.298:E1027-35, 2010.

34. **Chen J, Li J, Yiu JHC, Lam JKW, Wong CM, Dorweiler B, Xu A, Woo CW.** TRIF-dependent Toll-like receptor signaling suppresses Scd1 transcription in hepatocytes and prevents diet-induced hepatic steatosis. *Sci Signal*. 10 pii: eaal3336, 2017.

35. **Xiao F, Deng J, Guo Y, Niu Y, Yuan F, Yu J, Chen S, Guo F.** BTG1 ameliorates liver steatosis by decreasing stearoyl-CoA desaturase 1 (SCD1) abundance and altering hepatic lipid metabolism. *Sci Signal*. **9**: ra50, 2016.

36**. Mauvoisin D, Prévost M, Ducheix S, Arnaud MP, Mounier C.** Key role of the ERK1/2 MAPK pathway in the transcriptional regulation of the Stearoyl-CoA Desaturase (SCD1) gene expression in response to leptin. *Mol Cell Endocrinol*. 319: 116-28, 2010**.**

37. **Aljohani A, Khan MI, Syed DN, Abram B, Lewis S, Neill LO, Mukhtar H, Ntambi JM**. Hepatic Stearoyl-CoA desaturase-1 deficiency-mediated activation of mTORC1-PGC-1α axis regulates ER stress during high-carbohydrate feeding. *Sci Rep*. 9(1):15761, 2019.

Legends to figures

Figure 1: Repetitive AMD administration induces liver injury, steatosis and ER stress. Chronic injury was induced by administration by gavage of AMD (180mg.kg^{-1} body weight) for four consecutive days and the mice were sacrificed 24h later. (a) Serum ALT and AST. (b) Liver Oil Red O staining in mice with or without repetitive AMD treatment. Bar=100μm. (c) Expression of hepatic ER stress genes was detected by qRT-PCR and gene expression was normalized to *Rplp0*. (d) Western blots showing hepatic expression for ER stress proteins with p97 showing equal loading. Below is the densitometric quantitation. Results are expressed as averages ±SE. n=7-10, statistical significance between two groups was assessed by a two-tailed student t-test. Significance was set at *p <0.05.

Figure 2: Repetitive AMD induces ER stress in adipose tissue. C57Bl/6OlaHsd mice were used for the acute and repetitive AMD injury. The acute AMD injury by administration of one intraperitoneal injection of AMD (250 mg.kg^{-1} body weight). Chronic injury was induced by administration by gavage of AMD (180mg.kg^{-1} body weight) for four consecutive days. (a) Epididymal adipose tissue expression of genes involved in ER stress/ UPR was assessed by qRT-PCR and normalized to *Rplp0*. (b) Western blots show epididymal adipose tissue expression for ER stress proteins. Below is the densitometry analysis of the proteins normalized to housekeeping gene p97. (c) Epididymal adipose tissue expression of *Tnfa* assessed by qRT-PCR and normalized to *Rplp0*. Results are expressed as averages ±SE. n= 7-15. Statistical significance between two groups was assessed using a two-tailed student t-test. Significance was set at *p <0.05. Statistical significance between three groups was determined by one-way ANOVA, followed by Bonferroni's post hoc test, *p <0.05 significantly different from control group.

Figure 3: Repetitive AMD administration leads to lipolysis in adipose tissue *in vivo*, but inhibits lipogenesis. (a) Western blots showing epididymal adipose tissue expression of phosphorylated hormone sensitive lipase (pHSL). The right hand panel shows densitometry analysis of pHSL normalized to p97. (b) Serum FFA measured by ELISA. (c) Serum relative concentrations (mol%) of SFA and MUFA were determined with gas chromatography. Results are expressed as averages ±SE. n=4, *p <0.05. (d) Expression of lipogenesis-related genes was measured in the epididymal adipose tissue by qRT-PCR and normalized to *Rplp0*. (e) Western blot analysis of lipogenesis enzymes. The right hand panel shows densitometry analysis of the enzymes normalized to p97. Results are expressed as averages ±SE. n=10-12, statistical significance between two groups was assessed by a two-tailed student t-test. Significance was set at *p <0.05.

Figure 4: AMD treatment induces ER stress-dependent lipolysis in 3T3L1 differentiated into adipocytes. (a) Effect of various doses of 8 h of AMD treatment on the expression of ER stress/ UPR genes in 3T3L1 differentiated into adipocytes. Expression of the genes was assessed by qRT-PCR and normalized to *Rplp0*. (b) Effect of 100 μM AMD treatment on 3T3L1 adipocytes on ER stress/ UPR genes at different time points. Expression of the genes was assessed by qRT-PCR and normalized to *Rplp0*. (c) Effect of 100 μM AMD, with or without 50 μM BIX on 3T3L1 adipocytes ER stress/ UPR genes detected by qRT-PCR and normalized to *Rplp0*. (d) Free glycerol release from adipocytes in response to 100 μM AMD, with or without 50 μM BIX. Isoproterenol 1 μM was used as a positive control. Statistical significance between several groups was determined by one-way ANOVA, followed by Bonferroni's post hoc test, *p <0.05 significantly different from

control, #P < .05, significantly different from the BIX treatment, $^{@}$p <0.05 significantly different from AMD treatment.

Figure 5: Repetitive AMD administration causes hepatic FFA accumulation and increased expression of lipid uptake molecules: Concentrations of (a) Serum TAG, (b) Liver TAG. (c) Liver FFA measured by ELISA. (d) Expression of liver *Cd36* and *Fabp4* was determined by qRT-PCR and normalized to *Rplp0* housekeeping gene. (e) Western blot analysis shows protein levels of CD36 in livers of control and AMD- treated mice. The right hand panel shows densitometry of CD36 normalized to p97. All results are expressed as averages ±SE. Statistical significance between two groups was determined by a two-tailed student t-test. Significance was set at *p <0.05.

Figure 6: Repetitive AMD reduces hepatic expression of ELOVL6 and SCD1, accompanied by a decrease in their products palmitoleate (16:1n-7) and *cis*-vaccenate (18:1n-7) and increased lipotoxic palmitate (16:0). (a) Expression of lipogenesis-related genes was assessed in the liver by qRT-PCR and normalized to Rplp0 housekeeping gene. (b) Western blots showing hepatic expression of SCD1 and ELOVL6 protein. The right hand panel shows densitometry of the proteins normalized to p97 expression. (c) Relative concentrations (mol%) of hepatic SFA and MUFA were determined with gas chromatography. (d) TUNEL assay showing apoptosis in livers of AMD-treated mice. All results are expressed as averages ±SE. Statistical significance between two groups was determined by a two-tailed student t-test. Significance was set at *p <0.05.

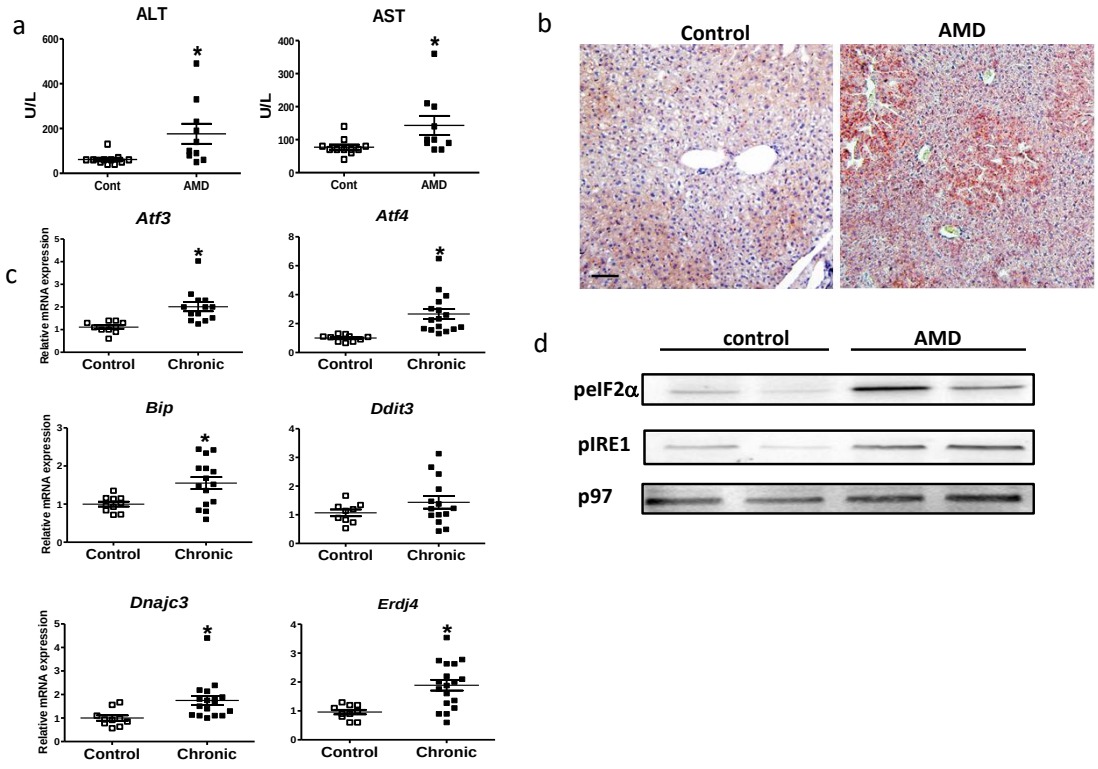
a
ALT
U/L
Cont
AMD
AST
U/L
Cont
AMD
c
Atf3
Relative mRNA expression
Control
Chronic
Atf4
Control
Chronic
Bip
Relative mRNA expression
Control
Chronic
Ddit3
Control
Chronic
Dnajc3
Relative mRNA expression
Control
Chronic
Erdj4
Control
Chronic
b
Control
AMD
d
control
AMD
peIF2α
pIRE1
p97

Fig.1

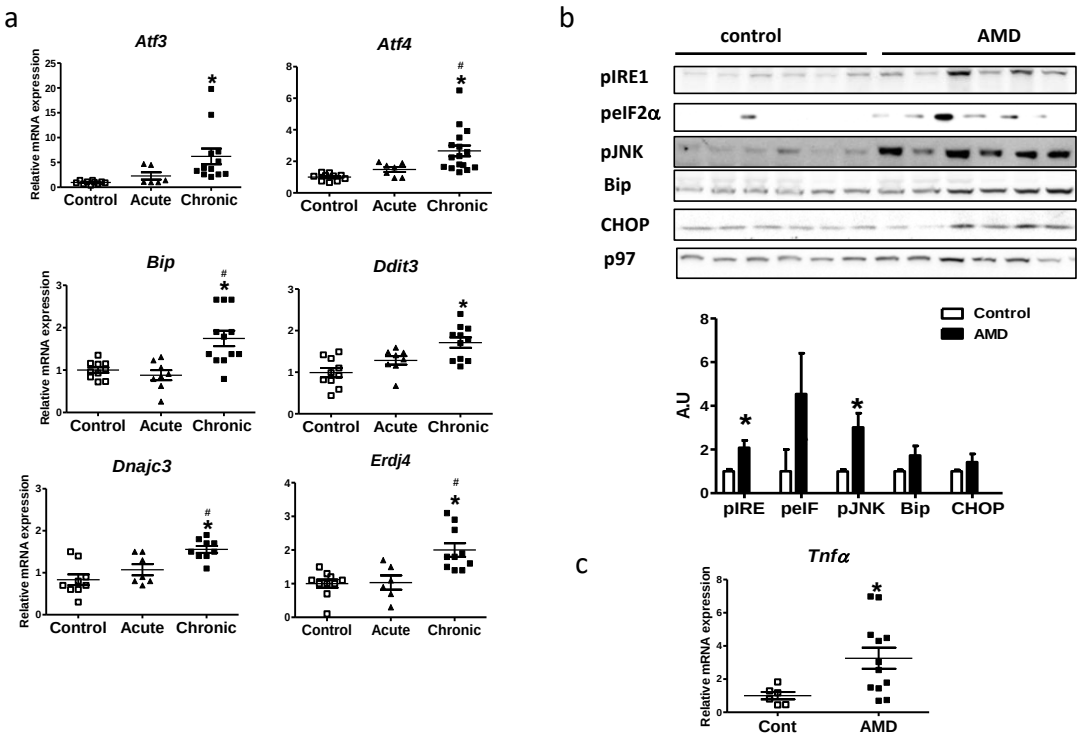
a
Atf3
Atf4
Bip
Ddit3
Dnajc3
Erdj4
Relative mRNA expression
Control
Acute
Chronic
b
control
AMD
pIRE1
peIF2α
pJNK
Bip
CHOP
p97
Control
AMD
A.U
pIRE
peIF
pJNK
Bip
CHOP
c
Tnfα
Relative mRNA expression
Cont
AMD

Fig.2

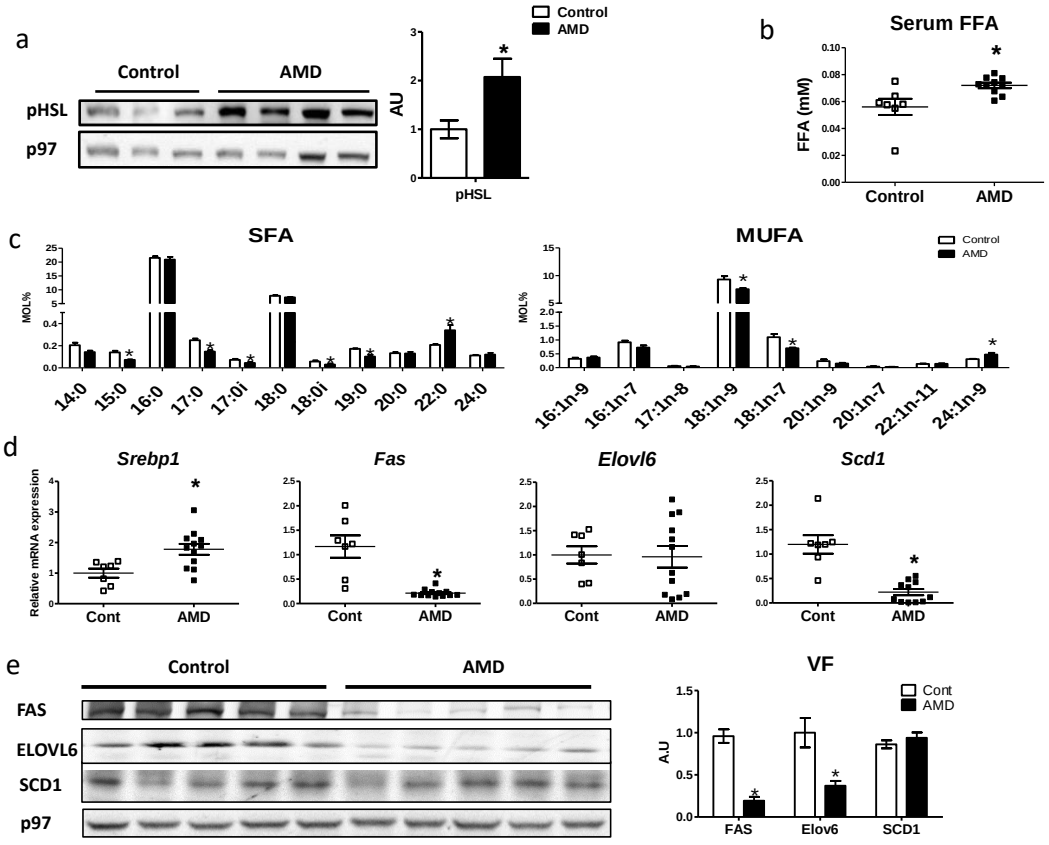
a
Control
AMD
pHSL
p97
AU
pHSL
b
Serum FFA
FFA (mM)
Control
AMD
c
SFA
MUFA
MOL%
14:0
15:0
16:0
17:0
17:0i
18:0
18:0i
19:0
20:0
22:0
24:0
16:1n-9
16:1n-7
17:1n-8
18:1n-9
18:1n-7
20:1n-9
20:1n-7
22:1n-11
24:1n-9
d
Srebp1
Fas
Elovl6
Scd1
Relative mRNA expression
Cont
AMD
e
Control
AMD
FAS
ELOVL6
SCD1
p97
VF
A.U
Cont
AMD
FAS
Elov6
SCD1

Fig.3

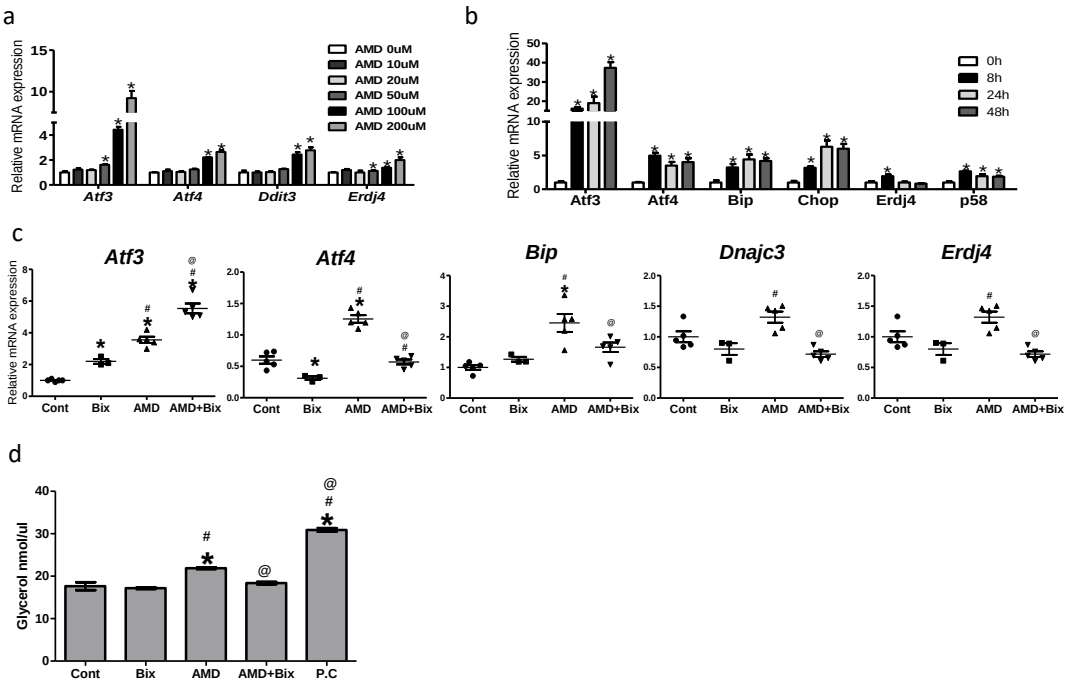
a
Relative mRNA expression
AMD 0uM
AMD 10uM
AMD 20uM
AMD 50uM
AMD 100uM
AMD 200uM
Atf3
Atf4
Ddit3
Erdj4
b
Relative mRNA expression
0h
8h
24h
48h
Atf3
Atf4
Bip
Chop
Erdj4
p58
c
Atf3
Atf4
Bip
Dnajc3
Erdj4
Relative mRNA expression
Cont
Bix
AMD
AMD+Bix
d
Glycerol nmol/ul
Cont
Bix
AMD
AMD+Bix
P.C

Fig.4

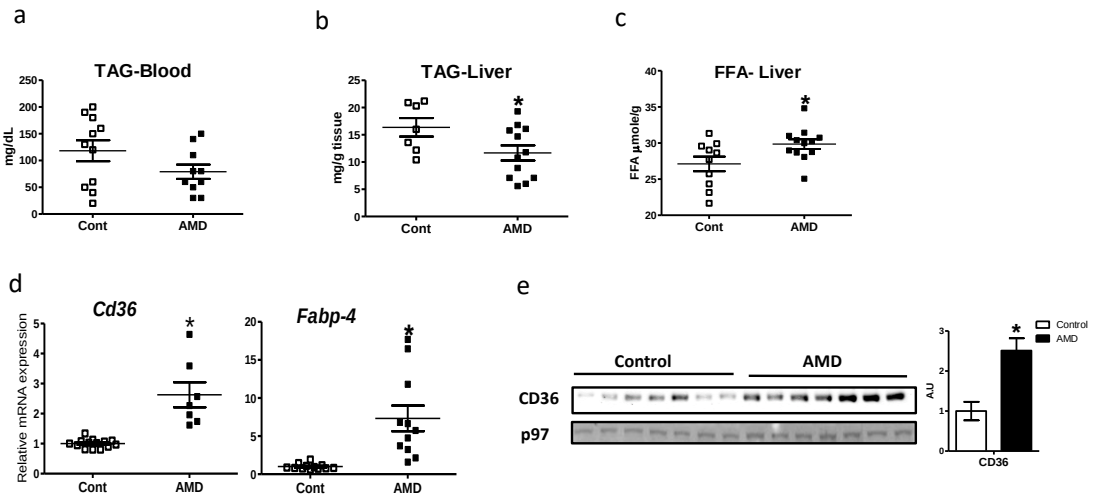
a
TAG-Blood
mg/dL
Cont
AMD
b
TAG-Liver
mg/g tissue
Cont
AMD
c
FFA- Liver
FFA µmole/g
Cont
AMD
d
Cd36
Relative mRNA expression
Cont
AMD
Fabp-4
Cont
AMD
e
Control
AMD
CD36
p97
AU
Control
AMD
CD36

Fig.5

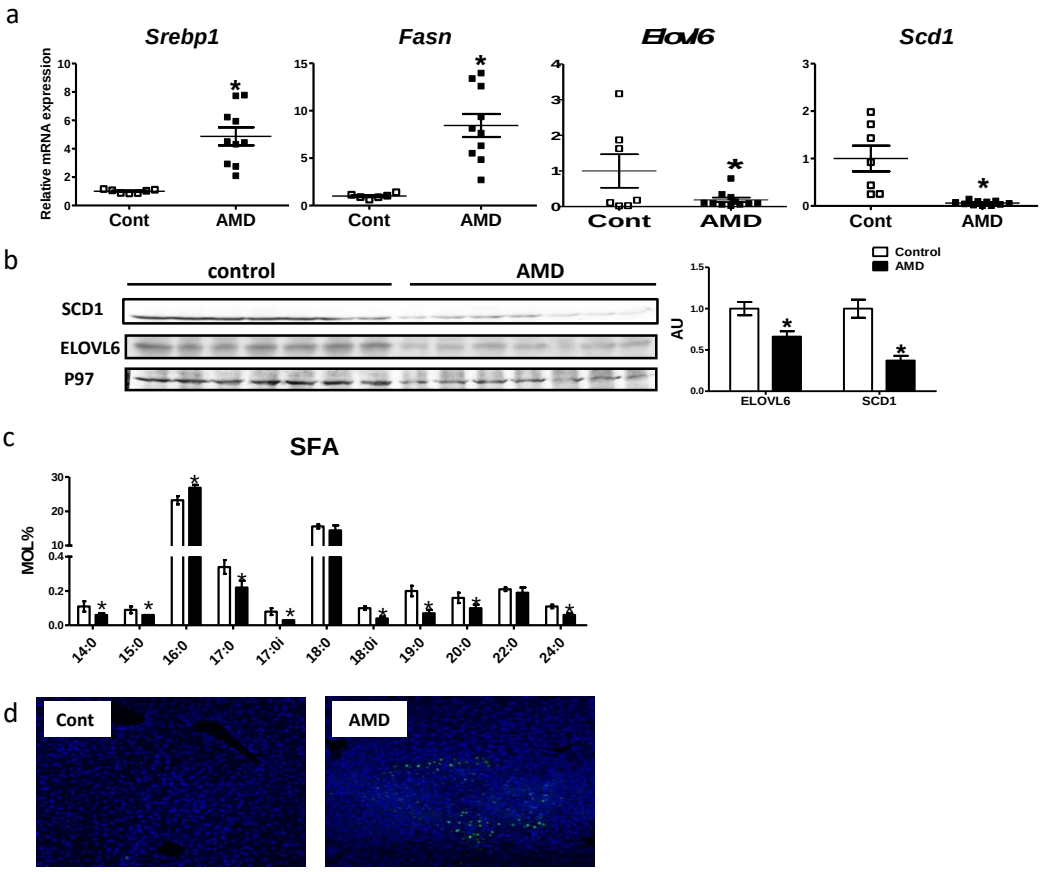
a
Srebp1
Fasn
Elovl6
Scd1
Relative mRNA expression
Cont
AMD
b
control
AMD
SCD1
ELOVL6
P97
Control
AMD
AU
ELOVL6
SCD1
c
SFA
MOL%
14:0
15:0
16:0
17:0
17:0i
18:0
18:0i
19:0
20:0
22:0
24:0
d
Cont
AMD

Fig.6